Simulations of a Triple Flame and Fire Whirl using the BIC Low-Mach-Number Algorithm

Xiao Zhang, Joseph D. Chung, Carolyn R. Kaplan, Elaine S. Oran
Department of Aerospace Engineering, University of Maryland
College Park, MD, USA

1 Introduction

Flames and other contact discontinuities introduce difficulties to numerical modeling of reactive flows due to the growth of numerical instabilities near these steep gradients. Over the past forty years, many high-order monotone algorithms have been developed to overcome these problems but were designed for explicit time integration methods. In this approach, the computational time-step is restricted by the sound speed and the convective velocity, ensuring numerical stability. Directly adopting these algorithms for low-speed flows, especially with chemical reactions, could be prohibitively expensive due to the wide disparity of time scales among the convective, acoustic, and chemical processes.

To overcome the computational difficulties, the low-Mach-number approximation of the Navier-Stokes equations was proposed. There are two main approaches in the development of algorithms for low Mach number flows. The first approach modifies compressible solvers, which aims to remove the sound speed restrictions in time-steps. Examples include the preconditioning methods [1] and the asymptotic approach [2]. The design of the former method is case dependent, and the latter method filters out the acoustic wave effects. The second approach uses a pressure correction to include the compressibility by extending an incompressible solver. A common method is the projection method which includes the SIMPLE family of algorithms [3] and also methods for reactive flows [4, 5]. Since the pressure and velocity are updated through an iterative process, these methods could suffer from slow convergence.

In a previous work [6], we applied a Barely Implicit Correction (BIC) [7] to the fourth-order Flux-Corrected Transport (FCT) [8] algorithm for nonreactive low-Mach-number flows. This approach first solves the full Navier-Stokes equations using a monotone algorithm with an explicit time integration as a prediction and then solves one elliptic equation for a pressure correction to eliminate the sound speed restriction in the time-step. This method maintains a low computational cost per time-step and preserves the effects of acoustic waves when needed. In [6], we demonstrated the ability of the BIC-FCT algorithm to remove the sound-speed limit in the numerical time-step for multidimensional nonreactive flow with complex swirling motions with and without open boundaries.

Correspondence to: xiaoz@terpmail.umd.edu

In this paper, we extend the BIC-FCT algorithm to compute reactive flows by modifying the integration procedure to include chemical reactions with heat release and physical diffusion processes. We present two cases. The simulation of a two-dimensional (2D) steady methane-air triple flame shows that the method can compute complex flame structures containing diffusion flames as well as rich and lean premixed flames. The simulation of an unsteady three-dimensional (3D) fire whirl demonstrates that the method can compute complex unsteady combustion in a turbulent swirling flow.

2 The Integration of BIC with a combustion model

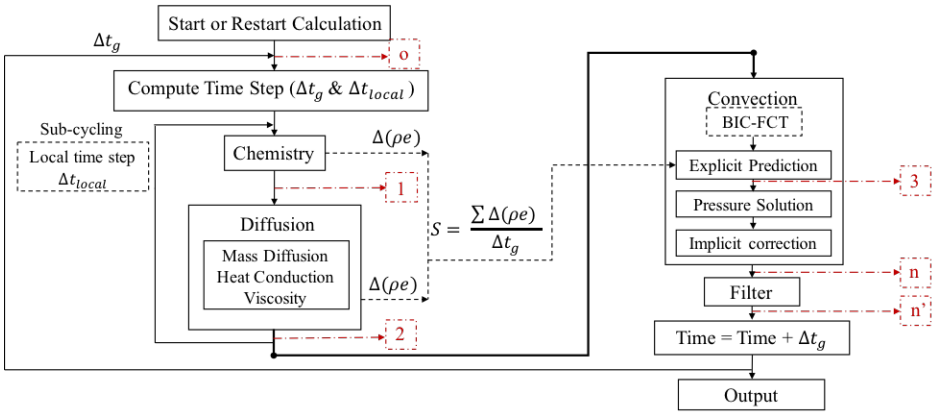

Figure 1: Flowchart of the coupling of the physical processes in one time-step

We solve the time-dependent, compressible, reactive Navier-Stokes (NS) equations using the recently developed BIC-FCT algorithm [6]. The temporal integration procedure including chemistry is shown in Fig. 1. This algorithm requires a process-splitting integration procedure. The first step is to compute the global time step, Δt_g, using the convective Courant-Friedrichs-Lewy (CFL) condition. Each of the diffusive processes, which include Fickian mass diffusion, Fourier heat conduction, and Newtonian viscosity, has its own explicit time-step limit due to numerical stability. We then compute these limits, including the limit for the reaction rate. The maximum reaction time-step is constrained by the amount of time required for a stoichiometric premixed flame to propagate through 10% of a computational cell. If the required time-steps from these non-convective processes are smaller than Δt_g, subcycling is applied for the integration of the chemistry and diffusion with a smaller time-step, Δt_{local}, using the minimum time-step limit of these non-convective processes.

Independently integrating the non-convective processes using the large time-step Δt_g allowed by BIC-FCT, even with subcycling, can produce unphysical results. More specifically, Δt_g can be so large that if the chemistry were integrated independently from the transport, the reaction can go from completely unburned to completely burned, unaffected by the other fluid processes. In reality, transport and reaction processes occur simultaneously within the flame. For example, the diffusion process pulls reactants into and away from the flame as the reaction occurs. Here, we reproduce this by first integrating chemistry for one small time-step, Δt_{local}, and then integrate the diffusion processes also for one Δt_{local}. The chemistry and diffusion are subcycled together in this way until the accumulated subcycling integration time reaches Δt_g. Also,

even with this subcycling procedure, there can be a large rise in pressure wherever the chemical energy is released because the compressible fluid processes have not redistributed the energy during the reaction. This rise is not an issue for explicit algorithms because the global time-step is the same order of magnitude as the chemical time-scale. To maintain constant pressure through the combustion process, the BIC algorithm removes the change in internal energy from non-convective processes and later redistributes it through the implicit correction stage. This change in internal energy is shown as S in Fig. 1 and is used in the same way as for nonreactive flows. This is explained in further detail in Section 3 of [6].

After integrating the chemical and diffusion processes, BIC performs an explicit prediction by explicitly solving the governing conservation equations using Euler explicit time-stepping and fourth-order FCT [8]. Then, one elliptic equation is solved to obtain a pressure correction. This pressure correction is used to correct the momentum and energy equations.

The effects of chemical heat release are included by using a calibrated chemical-diffusive model (CDM). Here, the CDM uses an Arrhenius function to regulate the conversion of reactant to product and the rate of heat release. In this model, three species are considered: fuel, oxidizer, and product. The chemical parameters are calibrated to reproduce the flame properties of heptane-air and methane-air mixtures for varying stoichiometry in a fluid dynamic computation. The CDM is a computationally inexpensive way to include the effects of chemical heat release in a computation. Details on this calibration procedure and the chemical parameters can be found in [9].

3 Applications

In this section, two test problems are shown to demonstrate the ability of the BIC-FCT algorithm to compute complex flame structures. The first problem is a two-dimensional, steady-state, methane-air triple flame and the second problem is a three-dimensional, unsteady, heptane-air fire whirl.

3.1 2D methane-air triple flame

A two-dimensional methane-air triple flame is simulated using a $16\ \mathrm{mm}$ square domain with an inflow-outflow boundary indicated in Fig. 2a. The top and bottom boundaries are symmetric. The flow is initialized with a stoichiometric ($\phi = 1$) methane-air laminar flame, shown by the temperature contour in Fig. 2(a). The inflow has a tanh mixture fraction profile as indicated by the line profile in Fig. 2(a). The inflow is stoichiometric at the center of the y-axis, fuel-rich approaching $\phi = 2$ along the upper y-axis, and fuel-lean approaching $\phi = 0$ along the lower y-axis. A coflow of inert gas is applied at the inflow within $2\ \mathrm{mm}$ of the upper and lower boundaries to avoid boundary effects. The inflow velocity is set to be $37.10\ \mathrm{cm/s}$, which is slightly smaller than the stoichiometric flame speed. This case is calculated on a 1024 $\times$ 1024 mesh using a convective CFL of 0.3.

The steady state flame temperature with superimposed heat release contours is shown in Fig. 2b. Most of the heat release is near the tip of the flame, around the stoichiometric region. Burning also occurs in the upper fuel-rich and lower fuel-lean regions. These regions are less reactive compared with the flame tip, which reduces the flame speed and results in the oblique flame structure. These oblique burning regions are premixed flames. They are not stoichiometric and there remains excess fuel and oxidizer after burning. The excess reactants then diffuse towards each other to form a diffusion flame, which is shown in Fig. 2b as the horizontal heat release contours.

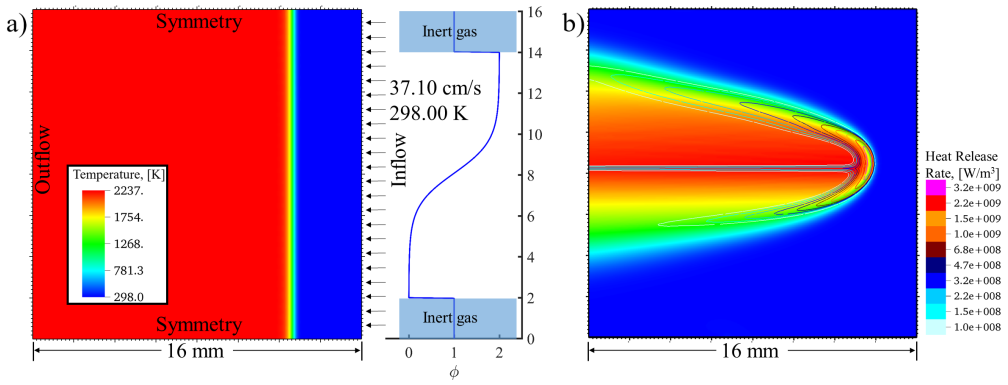

Figure 2: The (a) initial and boundary conditions and the (b) steady state temperature with superimposed heat release contours for a 2D methane-air triple flame simulation.

The temperature near the flame tip and in the horizontal diffusion flame region are near the adiabatic stoichiometric flame temperature, indicating that the pressure correction is correctly redistributing the energy in this complex 2D flowfield.

3.2 3D fire whirl

Fire whirls form when circulation couples with the hot, bouyant flow of burning material, generating swirling structures of hot gas. The flow field is highly unsteady and is tightly coupled to the diffusion and combustion processes. Therefore, we compute a 3D fire whirl to demonstrate that the BIC-FCT algorithm can compute complex, turbulent flow fields with chemical energy release.

A schematic of the geometrical setup and boundary conditions is shown in Fig. 3a. The domain is an enclosure with four walls which are $60\ \mathrm{cm}$ tall and $30\ \mathrm{cm}$ wide. The bottom floor is a $30\ \mathrm{cm} \times 30\ \mathrm{cm}$ square. Heptane vapor is injected at the center of the bottom floor with a constant velocity of $0.6\ \mathrm{cm/s}$ and temperature of $371\ \mathrm{K}$ within a diameter of $2.54\ \mathrm{cm}$. Air is forced in through the corners with a speed of $80\ \mathrm{cm/s}$ along slits which are $6\ \mathrm{cm}$ wide to apply circulation. The initial conditions are quiescent air with a temperature of $298\ \mathrm{K}$ and pressure of $1\ \mathrm{atm}$. A column of hot product gas with a temperature of $2500\ \mathrm{K}$ is placed in the center above the fuel inlet to provide a source for ignition.

Figure 3b shows a volume rendering of the stoichiometric mixture fraction contour after the flow has developed. In Fig. 4, we show the time-averaged temperature, axial velocity, and tangential velocity along the radial direction at different heights in the domain. Just above the floor as shown by the green and blue lines, the temperature profile has a slight 'V' shape with a lower temperature near the centerline. This is because of the fuel rich mixture within the core. Halfway up the domain, as indicated by the black line, the temperature at the center increases due to the heat transfer from the flame. The temperature inside the thermal core eventually develops a peak at the the center because of the flame contraction near the top, which is shown as the red line. At all heights, the tangential velocity profile exihibits solid body rotation within the thermal core and irrotational flow outside of it. The development of temperature and tangential velocity is qualitatively consistent with experimental measurents of fire whirls [10]. The axial velocity shows 'W' and 'V' shapes at lower heights, with local minima inside the thermal core. The axial velocity at the centerline

increases as the height increases because of buoyancy and attains a parabolic shape with the peak at the centerline. This agrees qualitatively with experimental measurements of fire whirls in other configurations and for other fuels [11].

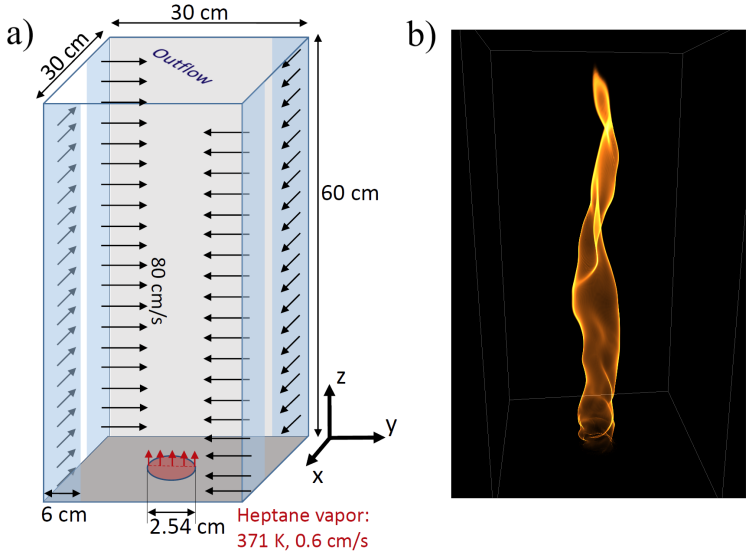

Figure 3: (a) Schematic of the geometrical setup and boundary conditions of a fire whirl computation. (b) Isometric view of a volume rendering of the stoichiometric mixture fraction isosurface.

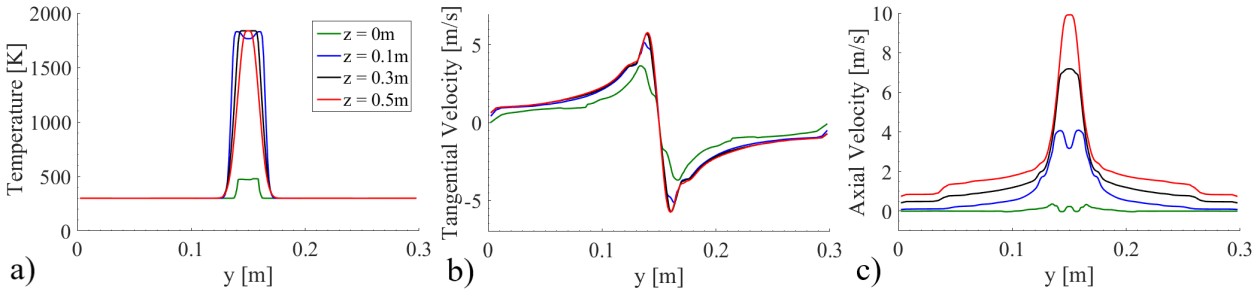

Figure 4: Time averaged (a) temperature, (b) tangential velocity, and (c) axial velocity radial profiles along different heights of the fire whirl computation.

3 Conclusions

In this work, we showed that BIC-FCT can compute complex flame structures and also obtain physically reasonable results when computing a complex 3D reactive flow. To do this, we extended the recently published low-Mach-number algorithm, BIC, to include chemistry. We described the BIC procedure with chemistry and diffusion processes. A 2D methane-air triple flame was simulated. The results showed that the algorithm is able to simulate a complex flame structure containing rich and lean premixed flames along with a diffusion flame. A 3D simulation of a fire whirl was also carried out to demonstrate the capability of

BIC-FCT to compute 3D, turbulent, swirling flows with chemical energy release. The radial profiles of temperature, tangential velocity, and axial velocity at different heights show qualitative agreement with other experimental measurements.

Acknowledgments

This work was supported by the Army Research Office (grant W911NF1710524) and by the National Science Foundation under award CBET 1839510. This work was also supported in part by the University of Maryland through Minta Martin Endowment Funds in the Department of Aerospace Engineering, and through the Glenn L. Martin Institute Chaired Professorship and the A. James Clark Distinguished Professorship at the A. James Clark School of Engineering. The authors gratefully acknowledge the fruitful discussions with Dr. Jay Boris and Dr. Gopal Patnaik at NRL. The authors also thank Dr. Ryan Houim of the University of Florida for assistance and guidance in the implementation of the numerical algorithms and many other helpful suggestions.

References

[1] Turkel E. (1987). Preconditioned methods for solving the incompressible and low speed compressible equations. J. Comput. Phys. 72: 277.

[2] Thornber B, Mosedale A, Drikakis D, Youngs D, Williams R.J. (2008). An improved reconstruction method for compressible flows with low Mach number features. J. Comput. Phys. 227: 4873.

[3] Patankar S. (1980). Numerical heat transfer and fluid flow. CRC press.

[4] Tomboulides AG, Lee JCY, Orszag SA. (1997). Numerical simulation of low Mach number reactive flows. J. Sci. Comput. 12: 139.

[5] Motheau E, Abraham J. (2016). A high-order numerical algorithm for DNS of low-Mach-number reactive flows with detailed chemistry and quasi-spectral accuracy. J. Comput. Phys. 313: 430.

[6] Zhang X, Chung JD, Kaplan CR, Oran ES. (2018). The barely implicit correction algorithm for low-Mach-Number flows. Comput. Fluids. 175: 230.

[7] Patnaik G, Guirguis RH, Boris JP, Oran ES. (1987). A barely implicit correction for flux-corrected transport. J. Comput. Phys. 71: 1.

[8] Boris JP, Landsberg AM, Oran ES, Gardner JH. (1993). LCPFCT- A flux-corrected transport algorithm for solving generalized continuity equations. NRL WASHINGTON DC, Tech. Rep.

[9] Chung JD, Zhang X, Kaplan CR, Oran ES. (2019). Low-Mach-Number Simulation of Diffusion Flames with the Chemical-Diffusive Model. In AIAA Scitech 2019 Forum, p.2169.

[10] Lei J, Liu N, Lozano JS, Zhang L, Deng Z, Satoh K. (2013). Experimental research on flame revolution and precession of fire whirls. Proc. Combust. Inst. 34: 2607.

[11] Hartl KA. (2016). Experimental investigation of laboratory fire whirls. Available at `http://arks.princeton.edu/ark:/88435/dsp01ng451k990`.